Comprehensive automatic assessment of retinal vascular abnormalities for computer-assisted retinopathy grading

Vinayak Joshi -*IEEE Member*, Carla Agurto -*IEEE Member*, Richard VanNess, Sheila Nemeth, Peter Soliz -*IEEE Member*, and Simon Barriga -*IEEE Member*

***Abstract* — One of the most important signs of systemic disease that presents on the retina is vascular abnormalities such as in hypertensive retinopathy. Manual analysis of fundus images by human readers is qualitative and lacks in accuracy, consistency and repeatability. Present semi-automatic methods for vascular evaluation are reported to increase accuracy and reduce reader variability, but require extensive reader interaction; thus limiting the software-aided efficiency. Automation thus holds a twofold promise. First, decrease variability while increasing accuracy, and second, increasing the efficiency.**

In this paper we propose fully automated software as a second reader system for comprehensive assessment of retinal vasculature; which aids the readers in the quantitative characterization of vessel abnormalities in fundus images. This system provides the reader with objective measures of vascular morphology such as tortuosity, branching angles, as well as highlights of areas with abnormalities such as artery-venous nicking, copper and silver wiring, and retinal emboli; in order for the reader to make a final screening decision. To test the efficacy of our system, we evaluated the change in performance of a newly certified retinal reader when grading a set of 40 color fundus images with and without the assistance of the software. The results demonstrated an improvement in reader's performance with the software assistance, in terms of accuracy of detection of vessel abnormalities, determination of retinopathy, and reading time. This system enables the reader in making computer-assisted vasculature assessment with high accuracy and consistency, at a reduced reading time.

I. Introduction

Cardiovascular disease (CVD), a common co-morbidity of diabetes mellitus (DM), is the number one cause of death among type 2 diabetics [1]. Signs of target end organ damage (TOD) caused by DM and CVD can be detected in the retina as hypertensive retinopathy (HR) [2]. Retinal vascular changes such as artery-venous (AV) nicking, copper and silver wiring, emboli, tortuosity, and changes in branching angle are reported to be associated with DM and CVD [3,4,5,6]. The features of HR can predict severity and risk of stroke and CVD, independent of blood pressure (BP) or its fluctuations, and even in patients with good BP control [7].

There is a dearth of eye care professionals to manage all of the patients at risk via traditional methods, especially in underserved areas. Introducing teleretinal screening allows primary care givers to provide access at a low cost. However, the inter-reader variability and qualitative nature of today's teleretinal screening settings create inefficiencies [8]. The inter-reader agreement for the detection of vascular abnormalities is only fair to moderate, such as κ=0.56 for AV nicking, and κ=0.42 for arterial narrowing [9,10], indicating high inconsistency in readers. Furthermore, intra-reader agreement of κ=0.34 indicates that readers often classify the same images in different categories. Several research groups have presented computer-assisted vascular analysis tools that are semi-automatic and address only a subset of vascular characteristics; such as the Diagnos CARA system [11], or IVAN [12,13]. These systems require extensive manual interaction in tracing of vessels or in classifying arteries and veins, and only measure artery-vein ratio, which takes up to 15 minutes; thus rendering them of limited utility for clinical use where real-time feedback is needed [12,13].

We present the first fully automated retinal vasculature analysis software as a second reader system, integrating the newly developed algorithms that provide vascular morphology measurements and vessel abnormality detection, to assist a reader in identifying the signs of retinopathy. This system allows a reader in making more accurate and consistent screening decisions with quantitative precision and quick turn-around time; which improves the cost effectiveness and efficiency of screening. This paper is organized as follows. Section II describes the methods and materials; Section III presents our results and discussion; finally, Section IV summarizes our conclusions.

II. Methods and Materials

A. System design

Fig. 1 shows the data flow and corresponding algorithms involved in the retinal image analysis. In the top row, the software sequentially processes a retinal image to produce a

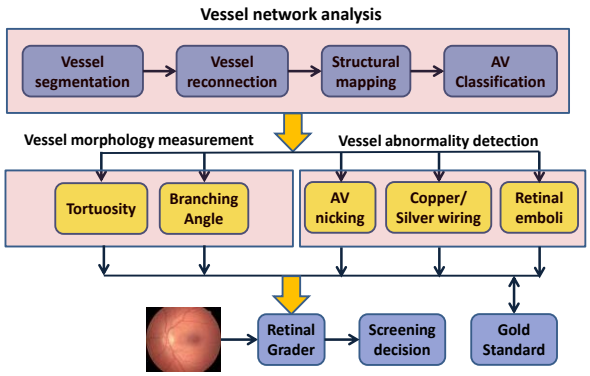

Figure 1: Flow chart of image processing steps.

Research supported by NIH - NEI grant 1R43EY024169-01.

Vinayak Joshi is with VisionQuest Biomedical LLC, Albuquerque, NM 87106 USA (corresponding author; phone: 505-508-1994; e-mail: vjoshi@visionquest-bio.com).

C. Agurto, R. VanNess, S. Nemeth, P. Soliz, and S. Barriga are with VisionQuest Biomedical LLC, Albuquerque, NM 87106 USA.

map of the vasculature using previously developed methods. In the middle row, the system uses our innovative algorithms that produce the features needed by the reader to determine a finding and make a grading decision.

B. Retinal vessel network analysis

The retinal vasculature assessment system was designed based on image analysis algorithms previously developed for vessel segmentation [14], segmentation correction by vessel reconnection [15], vessel tree separation by structural mapping [16,20], and artery-venous classification [17,18,20]. The performance of these algorithms was comparable to the relevant literature, and is reported in the cited publications. A brief description of these algorithms follows.

Vessel Segmentation: The segmentation algorithm [14] was developed based on illumination correction, multi-scale linear structure enhancement, and second order local entropy thresholding.

Vessel Reconnection: Image quality affects the quality of vessel segmentation resulting in interruptions, where a continuous vessel is often segmented into multiple disconnected vessel segments. This creates a false representation of vessel morphology. An algorithm was developed based on a method that identifies interruptions using connected component analysis and reconnects vessels using Dijkstra's graph search that determines a minimum cost path corresponding to the vessel ridges [15].

Structural Mapping: Vessel abnormality detection that is specific to a primary vessel and branching generations for both arteries and veins is needed for precise assessment of retinopathy [19]. However, the vessel trees are highly intertwined and complex for manual analysis. An algorithm was developed for remodeling the vessel trees into a vessel segment map and applying Dijkstra's graph search using vessel structural properties, to separate the vessel trees; as described in [20,16].

AV Classification: An algorithm was developed for artery-venous classification (Fig. 2) using a supervised classification method combined with vessel tree graph analysis [17]. This method uses multiple color and color variation features in the RGB, CIELab, YCbCr color spaces, as well as morphological features. A partial least squares (PLS) classifier is used to determine the probability that a vessel segment belongs to an artery or vein.

C. Retinal vessel abnormality detection

Detection of vessel abnormalities is highly predictive of hypertension and stroke [3,7]. We present the first fully automatic application that detects the vessel abnormalities and incorporates them into a computer-assisted system. The vessel network analysis methods form a foundation for newly developed algorithms for detecting various vessel abnormalities, described as follows. The ground truth was provided by a retinal specialist.

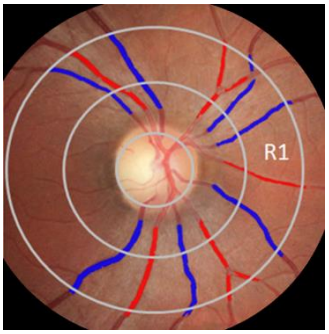

Figure 2. Automatic artery (red) – vein (blue) classification.

Vessel Morphology: The vascular morphology was measured in terms of vessel tortuosity and branching angle. An algorithm was developed based on a method for calculating tortuosity that formulates a tortuosity index (*TI, see equation below*) [21] comprising curved vessel length over its chord length (Lc/Lx), number of curvature sign changes (n), and magnitude of curvature (Θ).

The normal values of branching angle (72°) reflect an

$$TI = \frac{[n+1] * \sum_{i=1}^{m}[\theta i] * \sum_{i=1}^{m}[(Lci/Lxi)]}{Lc * m * m}$$

efficient blood transport [22], whereas the variations in branching angle may indicate atherosclerosis. During the structural mapping process [16,20], vessel properties such as vessel orientation are measured to separate the vessel trees by grouping vessel segments with similar properties. Therefore, branching angle is derived from the values of vessel orientation at each branching.

AV Nicking: A nicking or constriction of a vein by an artery at an artery-venous (AV) crossing (Fig. 3a-b) is indicative of hypertension [4]. Our system uses structural mapping to separate vessel trees and to detect the AV crossing points [16]. The vessel segments inside a region of interest (ROI, determined by image size) centered at each crossing point, are identified as arteries or veins using the AV classification [17,20]. The width of the vessel segments that is classified as a 'vein' inside the ROI, is then measured. AV nicking is identified when the average width of the vessel tip falls below 70% of the average width of rest of the vessel segment. Both proximal and distal tips of the vein segment are analyzed and the position of the vessel tips that fits the criterion for AV nicking is marked [10]. Twenty five fundus images were used to test the algorithm resulting in an accuracy of 82% against the ground truth, comparable to the accuracy of 88% reported in the literature [23].

Copper and Silver Wiring: With hypertension and atherosclerosis, arterial vessel walls thicken and the blood column color becomes less saturated, resulting in a shiny reflection of the arterial vessel wall known as copper and silver wiring (Fig. 4a). Our system uses a vessel reconnection method [15] to reconnect the interruptions in segmentation caused by copper or silver wiring, and AV classification

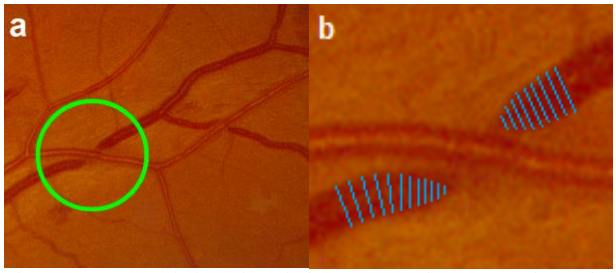

Figure 3. (a) Constriction of a vein by an artery. (b) Decreased vessel width profile, magnified view.

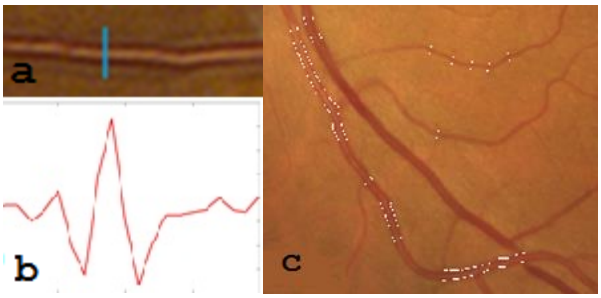

Figure 4. a) Copper wiring, b) Intensity profile at cross section, c) Wiring marked by white dots on vessel edges.

[17,20] method to identify arteries and veins. The presence of wiring is detected by analyzing the arterial cross-sectional intensity profile changing from vessel edges to vessel centerline (Fig. 4a-b), throughout the segmented artery length. The contrast between vessel edges and vessel centerline is enhanced by adaptive histogram equalization. The second order derivative of the equalized image is obtained, which describes the local vessel curvature and identifies the ridges formed by the presence of wiring. The arterial cross-sectional intensity profile in the derivative image is analyzed to determine a differential scalar value that represents the number of sign changes as well as the magnitudes of crests and troughs (Fig. 4b). A scalar value above an empirical threshold (representing a varying intensity profile) indicates the presence of copper or silver wiring, as marked by white dots on the vessel edges (Fig. 4c). The threshold is selected so as to differentiate between an arterial central reflex and presence of copper or silver wiring. The method was tested on 25 fundus images, yielding an accuracy of 71%.

Retinal Emboli (Hollenhorst Plaque): This abnormality presents as a bright yellow-colored flake trapped in an arterial bifurcation (Fig. 5a), and may indicate a risk of plaque formation in other blood vessels, e.g. carotid arteries, which could result in a stroke. However, there is no automatic application available that detects plaques in fundus images.

A plaque produces an intensity profile higher than retinal background and vessel section at bifurcation as shown in Fig. 5b. We use the method of structural mapping [16] to separate vessel trees, and to detect bifurcation points for the arterial vessel trees identified by AV classification [17,20]. The contrast between a potential plaque and retinal vessels is enhanced by adaptive histogram equalization in the ROI centered at each bifurcation point. The presence of a plaque is detected when the average intensity in a neighborhood of a bifurcation point (plaque region) is more than twice (empirical threshold) the average intensity of vessels inside the ROI. The method was tested on 15 fundus images, yielding an accuracy of 80%.

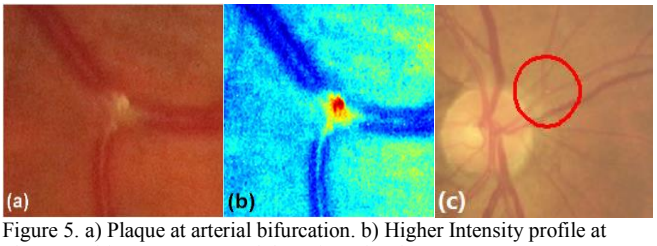

Figure 5. a) Plaque at arterial bifurcation. b) Higher Intensity profile at plaque position. c) Automated detection of a plaque

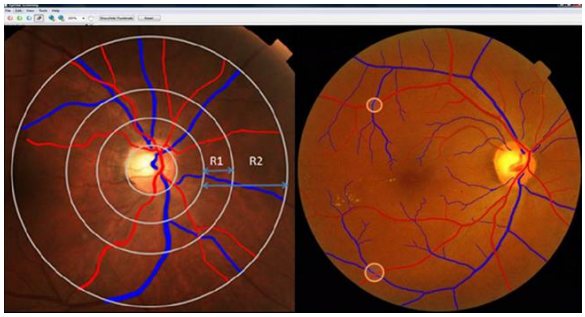

Figure 6: Example GUI showing abnormality detections

D. Evaluation of Reader's Performance.

A graphical user interface (GUI) was developed that integrates the algorithm findings, and used to aid the reader in a computer-assisted screening process. The GUI displays the input fundus image and the quantitative or visual data describing a particular vessel abnormality (Fig. 6). The measurements of morphological properties such as tortuosity and branching angle are displayed on the image beside to each individual vessel, or as an average value for the vessel network. The retinal regions with detected vascular abnormalities such as AV nicking, copper/silver wiring, and emboli are highlighted on the fundus image.

To evaluate the effect of the software in assisting a reader, a set of 40 standard two-field (optic-disc and fovea centered) fundus images was used consisting of 70% images with vascular abnormalities and 30% control images. The annotation of individual vessel abnormalities and overall determination of a retinopathy for each image, i.e. ground truth, was provided by a retinal specialist. A newly certified retinal reader with minimal grading experience analyzed each image for abnormalities and for the presence or absence of retinopathy, with and without the software assistance. The interval of 1 week between the two grading sessions offered an adequate memory-erase for the reader.

III. Results and Discussion

The reader's performance was calculated using the following metrics: 1) Sensitivity and number of false positives in identifying individual vascular abnormalities, 2) sensitivity and specificity in determining a retinopathy, and 3) average reading time required per image. Table I shows the comparison of reader performance with and without the assistance of the software system.

TABLE I. Effectiveness of Software-Assistance in Grading

Performance metric	Without software aid	With software aid
Sensitivity to abnormalities	57%	85%
No. of false positive abnormalities / Image	0.55	0.65
Sensitivity to retinopathy	81%	100%
Specificity to retinopathy	87%	100%

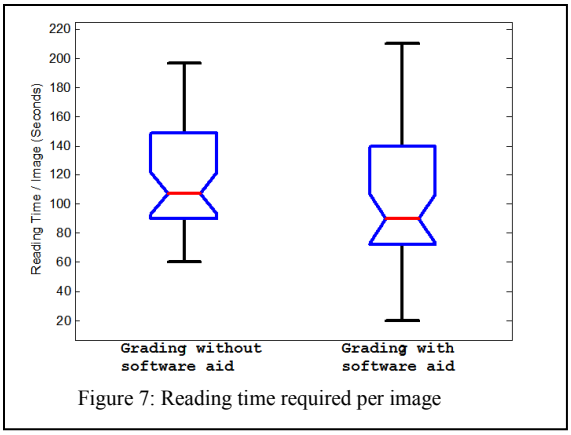

Figure 7: Reading time required per image

Our results demonstrate a significant increase in sensitivity in detecting vessel abnormalities, as well as increase in sensitivity and specificity in determining a retinopathy, when assisted with the software system.

However, the experiment reported a small increase in the number of false positive abnormality detections when assisted with the software, which is a result of over-detection by the software as well as the reader.

The increase in performance is further highlighted by an average reduction of 25 seconds in reading time which saves about quarter of the total reading time required per image (Fig. 7), due to the readily available vascular features provided by the software. Though the reading time with the software aid did not decrease significantly, the reader detected and annotated more abnormalities, resulting in greater than 25% of sensitivity.

Our study was based on images of sufficient quality for clinical determination and a large prevalence of vascular abnormalities. It is to be seen how image quality and image variation according to actual disease prevalence may affect our results. Also, we need to test the hypothesis that our system could be used as a learning tool for reading. As such it is conceivable that a reader learns from the system and becomes more adept at picking up vessel abnormalities.

IV. Conclusions

This work presents a novel software system, the first automated application that integrates the innovative algorithms developed for characterizing retinal vascular abnormalities, to aid human readers in computer-assisted screening of retinopathies. The results demonstrate a significant improvement in reader's performance in terms of accuracy and efficiency that could increase teleretinal screening throughput and point to more access. Better results in less time make a good economic argument for computer-assisted screening. We are in the process of conducting a clinical study with data collected at primary care settings to validate the algorithms and the system performance.

References

1 A. S. Go, D. Mozaffarian, V. L. Roger, D. M. Bravata, et al. "Heart Disease and Stroke Statistics—Update A Report From the American Heart Association." Circulation 127(1) (2013): e6–e245.

2 Y. Karter, A. Curgunlu, S. Altinişik, F. Ayan, et al. "Target Organ Damage and Changes in Arterial Compliance in White Coat Hypertension. Is White Coat Innocent?" Blood Pressure 12, no. 5–6 (2003): 307–313.

3 T. Y. Wong, R. Klein, D. J. Couper et al. "Retinal microvascular abnormalities and incident stroke: the Atherosclerosis Risk in Communities Study." Lancet 358, (2001), 1134–1140.

4 A. Joussen, T. Gardner, Retinal vascular diseases. Springer (2007)

5 M. Sasongko, J. Wang, N. Cheung, "Alterations in retinal microvascular geometry in young type 1 diabetes." Diabetes Care. (2010) 33(6).

6 M. Zamir, J. Medeiros, T. Cunningham, "Arterial bifurcations in the human retina." J. Gen. Physiol. 74 (1979) 537-548.

7 O. Yi-Ting, Y. T. Wong, R. Klein, Hypertensive Retinopathy and Risk of Stroke, *Hypertension*; 62:706-711; 2013.

8 T.Y. Wong, R. Klein, A.R. Sharrett, T.A. Manolio, L.D. Hubbard, E. K. Marino, L. Kuller, et al. "The Prevalence and Risk Factors of Retinal Microvascular Abnormalities in Older Persons: The Cardiovascular Health Study." Ophthalmology 110, no. 4 (April 2003): 658–666.

9 D.J. Couper, R. Klein, and F.J. Nieto. "Reliability of Retinal Photography in the Assessment of Retinal Microvascular Characteristics: The Atherosclerosis Risk in Communities Study." American Journal of Ophthalmology 133, no. 1 (2002): 78–88.

10 L.D. Hubbard, R.J. Brothers, W.N. King. "Methods for evaluation of retinal microvascular abnormalities associated with hypertension/ sclerosis in the Atherosclerosis Risk in Communities Study", Ophthalmology. 1999 Dec;106(12):2269-80.

11 CARA: Computer Assisted Retinal Analysis. http://www.diagnos.ca/cara/. Accessed 11/26/2013.

12 T.Y. Wong, M.D. Knudtson, R. Klein, and L.D. Hubbard, "Computer-assisted Measurement of Retinal Vessel Diameters in the Beaver Dam Eye Study: Methodology, Correlation Between Eyes, and Effect of Refractive Errors." Ophthalmology 111, no. 6 (2004): 1183–1190.

13 L.M. Sherry, J.J. Wang, E. Rochtchina, T.Y. Wong, R. Klein, L.D. Hubbard, and P. Mitchell. "Reliability of Computer-assisted Retinal Vessel Measurement in a Population." Clinical & Experimental Ophthalmology 30, no. 3 (2002): 179–182.

14 H. Yu, S. Barriga, C. Agurto and P. Soliz, "Fast Vessel Segmentation in Retinal Images Using Multiscale Enhancement and Second-order Local Entropy," Proc. SPIE 8315, (2012)

15 V. Joshi, M.K. Garvin, J.M. Reinhardt, M.D. Abramoff, "Identification and reconnection of interrupted vessels in retinal vessel segmentation", *IEEE, ISBI,* Image Segmentation Methods, FR-PS3a.7, p. 1416 - 1420, (2011).

16 V. Joshi, M.K. Garvin, J.M. Reinhardt, M.D. Abramoff, "Automated method for the identification and analysis of vascular tree structures in retinal vessel network", *SPIE Proceedings and conference*, Medical Imaging, vol. 7963, 79630I (2011).

17 H. Yu, S. Barriga, C. Agurto and P. Soliz, "Automated Retinal Vessel Type Classification in Color Fundus Images", *Proc SPIE*, 2013.

18 V. Joshi, M.K. Garvin, J.M. Reinhardt, M.D. Abramoff, "Automated artery-venous classification of retinal blood vessels based on structural mapping method", *SPIE Proceedings and conference*, Medical Imaging, vol. 8315, 83150I (2012).

19 M. Niemeijer, X. Xu, and M. Abramoff, "Automated measurement of the arteriolar-to-venular width ratio in digital color fundus photographs," IEEE TMI, vol. 30(11), pp. 1941 – 1950, 2011.

20 V. Joshi, J.M. Reinhardt, M.K. Garvin, M.D. Abramoff, Automated method for identification and artery-venous classification of Vessel Trees in Retinal Vessel Networks. (2014) PLoS ONE 9(2): e88061.

21 V. Joshi, J.M. Reinhardt, M.D. Abramoff, "Automated measurement of retinal blood vessel tortuosity", *Proc SPIE*, vol. 7624, 76243a (2010).

22 N. Witt, N. Chapman, S. Thom, "A novel measure to characterize optimality of diameter relationships at retinal vascular bifurcations" Artery Research 4(3) (September 2010) 75-80

23 U. Nguyen, A. Bhuiyan, L.A. Park, "An automated method for retinal arteriovenous nicking quantification from color fundus images, IEEE Trans Biomed Eng. 2013 Nov;60(11):3194-203.